Pergamon

Int. J. Solids Structures Vol. 34, No. 29, pp. 3873–3883, 1997

0020–7683/97 $17.00 + .00

PII: S0020–7683(96)00236–3

FRACTURE INITIATION AT SHARP NOTCHES: CORRELATION USING CRITICAL STRESS INTENSITIES

MARTIN L. DUNN, WAN SUWITO
Center for Acoustics, Mechanics, and Materials, Department of Mechanical Engineering, University of Colorado, Boulder, CO 80309-0427, U.S.A.

and

SHAWN CUNNINGHAM
Ford Microelectronics, Inc., Colorado Springs, CO 80921, U.S.A.

(*Received* 19 *June* 1996; *in revised form* 6 *November* 1996)

Abstract—In the context of linear elasticity, a stress singularity of the type $K^n r^\delta$ ($\delta < 0$) may exist at sharp re-entrant corners, with an intensity K^n. The magnitude of the intensity fully characterizes the stress state in the region of the corner. A critical value of K^n may be appropriate as a failure criterion in situations where the region around the corner dominated by the singular field is large compared to intrinsic flaw sizes, inelastic zones, and process zone sizes. We determined K^n for notched mode I three-point flexure specimens using a combination of the Williams (Williams, M. L. (1952) Stress singularities resulting from various boundary conditions in angular corners of plates in extension. *Journal of Applied Mechanics* **74**, 526–528) asymptotic method, dimensional considerations, and detailed finite element analysis. We carried out an experimental study of the feasibility of using a critical value of K^n to correlate failure with a series of notched polymethyl methacrylate (PMMA) three-point flexure specimens with notch angles of 60°, 90°, and 120°. Using the measured failure loads and the finite element solutions for K^n, we infer the critical notch stress intensity K^n_{cr} for sharp-notched PMMA. The data show that excellent failure correlation is obtained through the use of the single parameter K^n_{cr}. Furthermore, simple estimates of the size of the inelastic zone for the notched PMMA specimens show it to be small relative to the singularity-dominated zone. This supports the applicability of linear elastic notch mechanics (LENM), and the idea that a critical value of K^n can be used to correlate fracture initiation. © 1997 Elsevier Science Ltd.

1. INTRODUCTION

The prediction of brittle fracture in cracked solids based on the stress intensity factor K of linear elastic fracture mechanics is widely accepted. The suitability of using the single parameter K to correlate fracture is a result of the universal nature of the singular stress field near a crack tip as shown by Williams (1952). Williams further showed that a universal singular stress field of the form $\sigma_{\alpha\beta} = Kr^{\lambda-1}f_{\alpha\beta}(\theta)$ also exists in the region surrounding a sharp notch. In fact, the case of a crack is really an extreme case of a re-entrant notch where the included angle is zero. In the expression for the universal stress field, $\lambda - 1$ is the order of the stress singularity. It, along with the angular function $f_{\alpha\beta}(\theta)$, can be completely determined by an asymptotic analysis of the stress state. Thus, they are not functions of the particular geometry of the solid containing the notch or the specific far-field loading. The stress intensity K is a function of the geometry of the solid and the far-field loading, and thus for a given geometry and loading, K completely characterizes the stress state in a region near the notch tip.

Since Williams' (1952) pioneering work, numerous studies have been undertaken to determine the order of the stress singularity $\lambda - 1$ for various notch geometries. These include a large number of studies directed toward isotropic single and multiple-phase wedge/notch geometries (see Dempsey and Sinclair (1981) for an extensive list of references). In addition, stress singularities in anisotropic media have been extensively studied using analytical (Ting and Chou, 1981; Ting, 1986) and numerical (Sukumar and Kumosa, 1992;

Gu and Belytchko, 1994) approaches in anisotropic elasticity. The motivation for the studies in anisotropic elasticity has to a large degree been the study of singular stress fields in composite materials. Despite the numerous studies directed toward obtaining $\lambda-1$, very few studies have focused on obtaining the corresponding stress intensity K for a specific geometry. In fact, we know only of the works of Leicester (1973), Walsh (1974; 1976), Gross and Mendelson (1972), Sinclair *et al.* (1984), Knesl (1991), and Dunn *et al.* (1996).

As in linear elastic fracture mechanics, it seems reasonable that given the universal singular stress field around the notch tip, it may be possible to correlate fracture initiation at sharp notches with a critical value of the stress intensity. This critical value is a parameter that describes fracture initiation under a very complicated stress state, namely the universal singular stress state. Only a few studies have addressed the suitability of using a critical K for a non-zero notch angle to correlate fracture initiation. Carpinteri (1987) performed three-point flexure tests with notched PMMA bars and attempted to experimentally obtain the connection between a critical stress intensity at various angles and structure sizes. Although it may be possible to empirically correlate the critical stress intensity at various angles, it may not be formally appropriate because even though for a given notch angle the asymptotic stress field is universal, the universal field differs for different angles. Of course, only for the limiting case of a crack is there a rigorous connection between the stress intensity factor and the energy release rate of fracture mechanics. Thus a critical K failure criterion is suitable only for fracture initiation. Additional support for an approach to correlate fracture initiation based on the intensity of an elastic singularity other than that for a crack is provided by the recent studies of Reedy (1990; 1991; 1993a,b) and Reedy and Guess (1993; 1995; 1996). They correlated failure of adhesive-bonded butt tensile joints with a generalized stress intensity at the free edge of an interface corner between elastic and rigid layers. In their studies the order of the elastic singularity is about $\lambda-1=-1/3$ as compared to $\lambda-1=-1/2$ for a crack.

The success of these approaches has motivated us to attempt to use a critical stress intensity at reentrant notch corners to correlate failure of micromachined silicon structures which often poses sharp corners due to the fabrication by crystallographic etching. In this study, we present our initial efforts to this end. In Section 2 we apply the asymptotic analysis of Williams (1952) to determine the order of the elastic singularity and the angular dependence of the stress and displacement fields at a sharp notch. These fully determine the stress state at the notch tip within an arbitrary constant, the notch stress intensity K^n, which is a function of the geometry of the structure and the loading. In Section 3 we obtain K^n by detailed finite element calculations for notched three-point flexure specimens proposed to obtain a critical value of K^n. We present an experimental study carried out on notched polymethyl methacrylate (PMMA) three-point flexure specimens in Section 4. The extraction of a critical K^n is discussed in Section 5, along with a discussion of its suitability to correlate fracture initiation at sharp notches, followed by concluding remarks in Section 6.

2. ASYMPTOTIC ANALYSIS OF SINGULAR FIELDS

Consider the notched body shown in Fig. 1. It is loaded by tractions on remote boundaries and the surfaces $\theta=\pm\alpha$ are traction free. In the following we redundantly, but conveniently, refer to γ as the notch angle where γ is related to α by $\gamma/2=\pi-\alpha$. For simplicity we assume linear isotropic material behavior. The asymptotic, possibly singular, fields near the notch tip can be obtained using Williams (1952) eigenfunction expansion method for both the plane and antiplane problems. For the plane problem, the appropriate Airy stress function is:

$$\phi = r^{\lambda+1} f(\theta) \tag{1}$$

where:

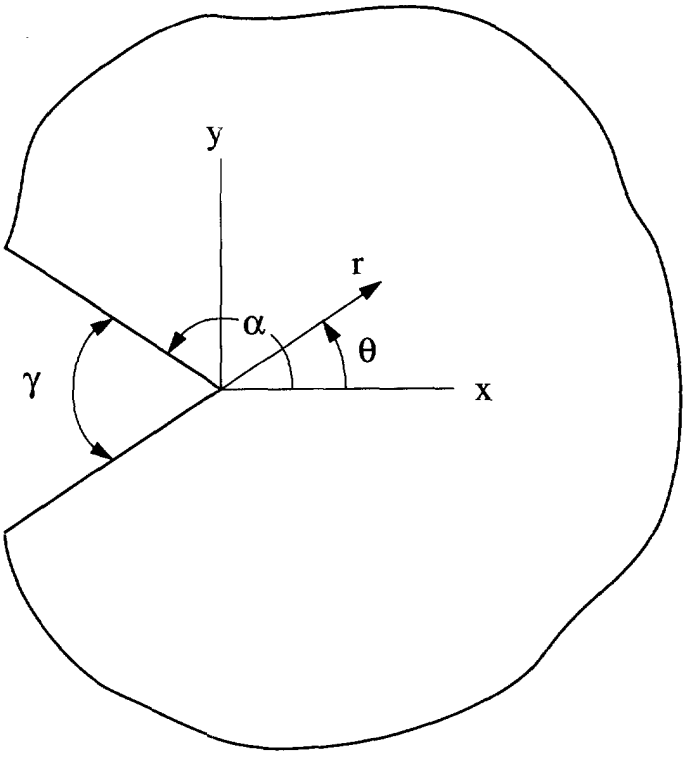

Fig. 1. Geometry of the corner considered in this study.

$$f(\theta) = A_1 \cos(\lambda+1)\theta + A_2 \sin(\lambda+1)\theta + A_3 \cos(\lambda-1)\theta + A_4 \sin(\lambda-1)\theta. \tag{2}$$

In the standard manner, the stresses can be obtained from ϕ as:

$$\begin{aligned} \sigma_{rr} &= r^{\lambda-1}[(\lambda+1)f(\theta)+f''(\theta)] \\ \sigma_{\theta\theta} &= r^{\lambda-1}\lambda(\lambda+1)f(\theta) \\ \sigma_{r\theta} &= -r^{\lambda-1}\lambda f'(\theta). \end{aligned} \tag{3}$$

Note that $\lambda > 0$ for boundedness of the strain energy and $\lambda < 1$ for singular fields. Imposing traction-free boundary conditions on $\theta = \pm\alpha$ results in a system of four equations for the five unknowns A_i and λ. A nontrivial solution requires that the determinant of the coefficient matrix vanish. Upon imposing this requirement, two equations result, one for symmetric fields with respect to the x-axis ($\theta = 0$), and one for antisymmetric fields. For the symmetric, or mode I, fields:

$$\lambda \sin 2\alpha + \sin 2\lambda\alpha = 0. \tag{4}$$

The order of the mode I singularity λ is tabulated in Table 1 as a function of γ.

Table 1. Order of the corner stress singularity and coefficients of the nondimensional function $f(a/h)$ in eqn (8) for the notched three-point flexure specimens

γ (degrees)	λ	c_1	c_2	c_3	c_4	c_5
0	0.5000	3.99812	−24.5978	84.3671	−129.951	77.8949
60	0.5122	4.45310	−27.9941	96.0504	−147.987	88.3623
90	0.5445	5.45245	−35.6525	122.909	−189.630	112.681
120	0.6157	7.89944	−55.2765	193.464	−300.322	177.660

Once λ is obtained from eqn (4), the coefficients A_i can be expressed in terms of a single A_i. We normalize the system so that $\sigma_{\theta\theta}(\theta = 0) = K_I^n r^{\lambda-1}$. This allows us to write the mode I singular stresses and displacements as:

$$\begin{aligned}\sigma_{\alpha\beta} &= K_I^n r^{\lambda-1} f_{\alpha\beta}(\theta)\\ \sigma_m &= K_I^n r^{\lambda-1} f_m(\theta)\\ \sigma_e &= K_I^n r^{\lambda-1} f_e(\theta)\\ u_\alpha &= K_I^n r^{\lambda} g_\alpha(\theta).\end{aligned} \tag{5}$$

In eqns (5) α and β take on the values (x, y, z) in Cartesian coordinates and (r, θ, z) in cylindrical coordinates. The subscript α is not to be confused with the angle α. σ_e is the von Mises effective stress and σ_m is the mean stress. They are computed from $\sigma_{\alpha\beta}$ in the standard manner. $\lambda, f_{\alpha\beta}(\theta), f_m(\theta), f_e(\theta)$, and $g_\alpha(\theta)$ are determined by the asymptotic analysis. λ and $f_{\alpha\beta}(\theta)$ $(\alpha, \beta \neq 3)$ are functions only of α, while $f_m(\theta), f_e(\theta)$ and $g_\alpha(\theta)$ are functions of α and the elastic properties of the material. $f_{33}(\theta)$ is a function of α and Poisson's ratio and differs depending on whether plane strain or plane stress conditions are assumed. The stress intensity K_I^n is a function of the specific geometry and loading. Its magnitude fully determines the stress state at the notch tip for a given notch angle γ (or α).

3. FINITE ELEMENT SOLUTION FOR K^n: NOTCHED THREE-POINT FLEXURE SPECIMENS

We focus on a specimen designed to determine a critical value of the mode I stress intensity factor K_I^n. We emphasize mode I because the singularity is much stronger than that for mode II for geometries and loadings of practical interest and so mode I failure is thought to dominate. For example, for a notch angle of $\gamma = 90°$, $\lambda - 1 = -0.4555$ and -0.0915 for modes I and II, respectively. The specimen studied here, a notched three-point flexure specimen, is shown in Fig. 2, along with typical loading.

Dimensional considerations lead to the following form for K_I^n:

$$K_I^n = \sigma^0 h^{1-\lambda} f\left(\frac{a}{h}\right) = \left(\frac{3PL}{2bh^2}\right) h^{1-\lambda} f\left(\frac{a}{h}\right). \tag{6}$$

The order of the singularity λ is determined from the asymptotic analysis and all other parameters except the dimensionless factor $f(a/h)$ are known for a specified geometry and

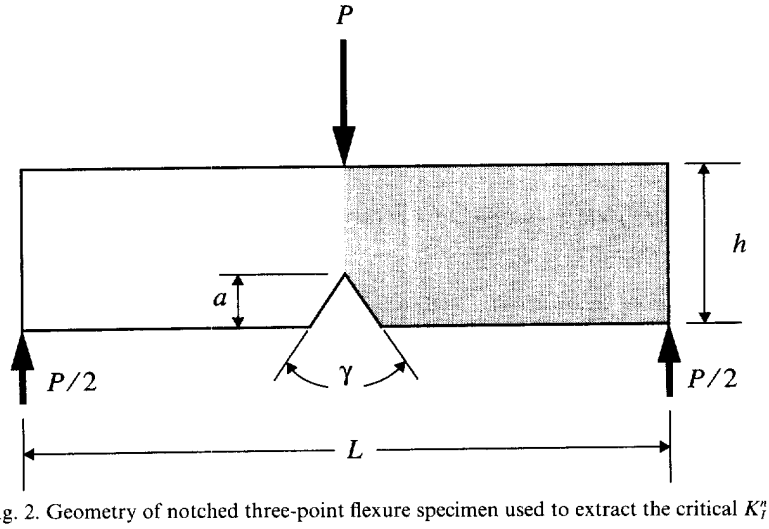

Fig. 2. Geometry of notched three-point flexure specimen used to extract the critical K_I^n.

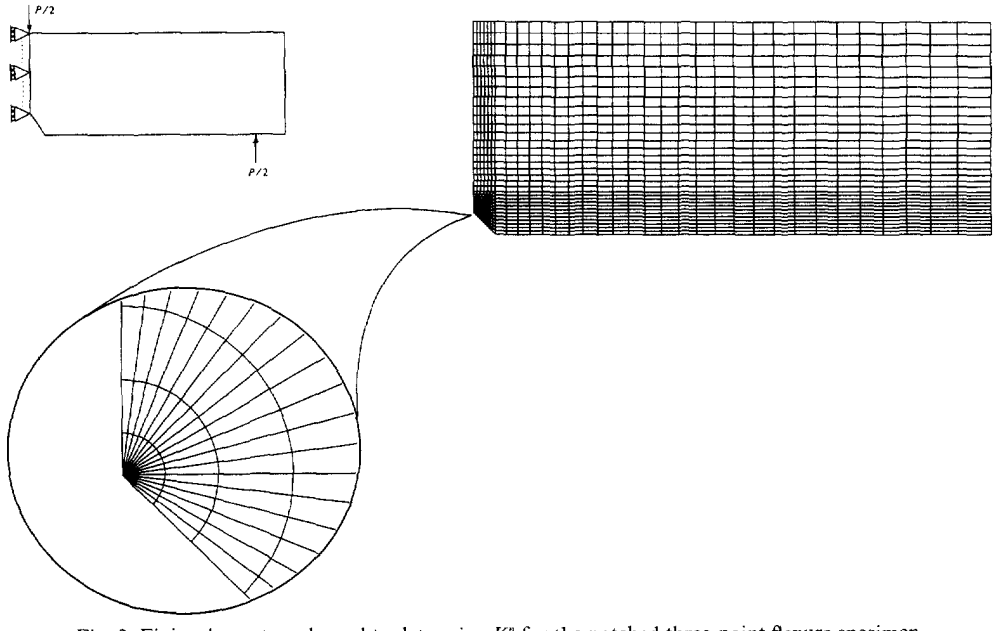

Fig. 3. Finite element mesh used to determine K_I^n for the notched three-point flexure specimen.

loading. Values of λ for various notch angles γ are tabulated in Table 1. We performed plane strain finite element calculations to determine the dimensionless factor $f(a/h)$, and to obtain full-field solutions for the notched flexure specimens. A representative mesh is shown in Fig. 3 for $\gamma = 90°$, along with the appropriate boundary conditions. Near the corner we use a highly-refined mesh in order to accurately determine K_I^n. The mesh shown in Fig. 3 contains 1308 8-node quadratic elements and 8032 degrees of freedom. Meshes for other notch angles are similar.

We can determine K_I^n by correlating either calculated stresses or displacements with the asymptotic formula of eqn (5) as is done in computational fracture mechanics. Because they are more accurate than computed stresses, we use calculated nodal displacements to determine K_I^n. Specifically, we used the displacement component u_y along the notch flanks, $\theta = \pm\alpha$. K_I^n was determined from a least-squares fit (to find C) of:

$$u_y(\theta = \alpha) = Cr^{\lambda} \tag{7}$$

where again λ is determined from the asymptotic analysis. K_I^n was then computed from $K_I^n = C/g_y(\theta = \alpha)$ where $g_y(\theta = \alpha)$ is also determined from the asymptotic analysis. A plot of $u_y(\alpha)$ vs r is shown in Fig. 4 for the various values of a/h for the $\gamma = 90°$ specimen. The results for specimens with other notch angles are similar. With K_I^n so determined, we computed $f(a/h)$ from eqn (6). For the range of $0.05 \leqslant a/h \leqslant 0.7$, $f(a/h)$ can be fit by the polynomial:

$$f\left(\frac{a}{h}\right) = c_1\left(\frac{a}{h}\right) + c_2\left(\frac{a}{h}\right)^2 + c_3\left(\frac{a}{h}\right)^3 + c_4\left(\frac{a}{h}\right)^4 + c_5\left(\frac{a}{h}\right)^5. \tag{8}$$

Results for the constants c_i are given in Table 1 for the range of notch angles studied.

4. NOTCHED THREE-POINT FLEXURE TESTS

We carried out a series of tests with notched three-point flexure specimens to determine the suitability of using a critical value of K_I^n to correlate failure at sharp notches. Notched flexure specimens (Fig. 2) were machined from polymethyl methacrylate (PMMA) with dimensions of $L = 76.2$ mm, $b = 12.7$ mm, $h = 17.8$ mm. Specimens were machined with

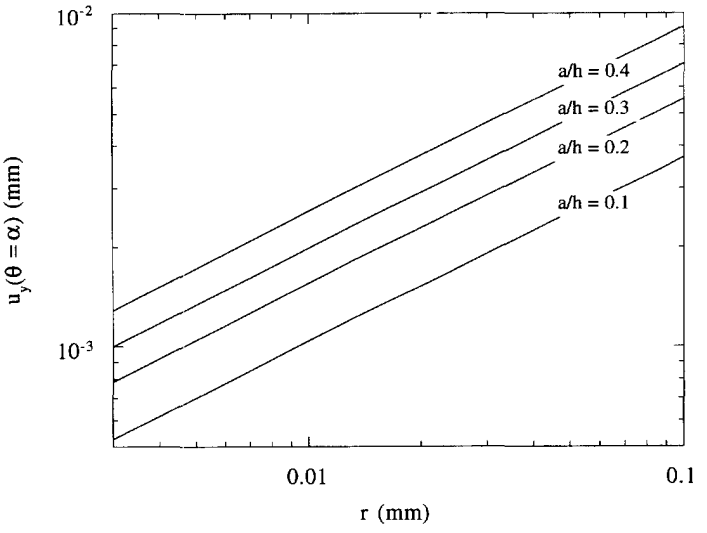

Fig. 4. Displacement u_y along the notch flank $\theta = \alpha$ for the edge-notched specimens for $\gamma = 90^\circ$ at various values of a/h with $h = 17.8$ mm.

three notch angles: $\gamma = 60^\circ$, 90°, and 120°. For each notch angle four notch depths were used: $a = 1.78$, 3.56, 5.33, and 7.11 mm. These result in a/h ratios of 0.1, 0.2, 0.3, and 0.4, respectively. The notch was carefully machined to yield a notch-tip radius less than 0.0254 mm. The notch tip radius was far less than 0.0254 mm for the $\gamma = 90^\circ$ and 120° specimens and right at that value for $\gamma = 60^\circ$. Optical microscopy revealed no evidence of crazing ahead of the notch tip such as that observed in cracked PMMA (Williams, 1984).

We measured the elastic moduli and the uniaxial stress-strain curve of the PMMA with a standard tensile test at a strain rate of 8.75×10^{-4}/s. The stress-strain response is well-described by a combination of a Ramberg-Osgood (linear plus power-law hardening) model from $0 \leqslant \varepsilon \leqslant 0.0625$, and a perfectly-plastic model for $0.0625 \leqslant \varepsilon \leqslant 0.086$ where 0.086 is the failure strain. The Ramberg-Osgood model is described by:

$$\varepsilon = \frac{\sigma_y}{E}\left(\frac{\sigma}{\sigma_y} + \chi\left(\frac{\sigma}{\sigma_y}\right)^n\right). \tag{9}$$

Young's modulus is $E = 2.3$ GPa, and although we did not measure Poisson's ratio, a detailed study by Ledbetter (1996) shows that it is 0.36. In addition to E, the fitting parameters in eqn (9) are $\sigma_y = 51$ MPa, $\chi = 0.164$, and $n = 6.5$.

We also measured the plane strain fracture toughness of the PMMA using cracked three-point flexure specimens with the same dimensions given above, following the procedures outlined in ASTM E-399, the Standard Test Method for Plane-Strain Fracture Toughness of Metallic Materials. The cracks were formed by sawing a thin notch to a depth of about 2 mm, and then using a sharp razor blade to drive a crack to a nominal depth of about 10 mm ($a/h \sim 0.5$). The flexure specimen was loaded at a crosshead displacement rate of 0.1 mm/s. The average measured fracture toughness of four specimens is 1.02 MPa $\sqrt{\text{m}}$ with a standard deviation of 0.12 MPa$\sqrt{\text{m}}$ (standard deviation/average = 11.8%). This scatter is in line with typical values for well-cracked specimens (Williams, 1984).

Flexure tests were performed with the notched specimens in an Instron servo-hydraulic machine. The specimens were loaded at a crosshead displacement rate of 0.10 mm/s. The results show linear load-displacement response, followed by brittle fracture. Examination of the failed specimen indicates crack propagation along the symmetric plane ahead of the notch tip. The failure surface is nearly perfectly smooth, exhibiting a mirror-like finish. It contains very fine lines that run perpendicular to the notch front and show brilliant colors. These lines appear to be the same as those reported in tests of cracked PMMA and have been interpreted as interference effects of incident white light being reflected from layers of

oriented molecules (Higuchi, 1958; Berry, 1961). Failure stresses for each test are tabulated in Tables 2–5. The failure stress is defined as the stress σ^0 in eqn (6) as computed using the measured failure loads. We also performed flexure tests on unnotched specimens and found the average failure stress to be $\sigma_f = 124$ MPa with a standard deviation of 20 MPa.

Table 2. Failure strength and critical K_I^n for the notched three-point flexure specimens with $a = 1.78$ mm ($a/h = 0.1$)

	$\gamma = 60°$		$\gamma = 90°$		$\gamma = 120°$	
	σ_f (MPa)	K_{Ic}^n (MPa · m$^{0.4878}$)	σ_f (MPa)	K_{Ic}^n (MPa · m$^{0.4555}$)	σ_f (MPa)	K_{Ic}^n (MPa · m$^{0.3843}$)
	16.97	0.569	19.63	0.887	24.85	2.031
	17.41	0.584	19.63	0.887	25.17	2.057
	17.35	0.582	19.31	0.873	25.01	2.044
	17.41	0.584			25.17	2.057
Avg.	17.29	0.580	19.52	0.882	25.05	2.047
St. Dev.	0.21	0.007	0.18	0.008	0.15	0.012

Table 3. Failure strength and critical K_I^n for the notched three-point flexure specimens with $a = 3.56$ mm ($a/h = 0.2$)

	$\gamma = 60°$		$\gamma = 90°$		$\gamma = 120°$	
	σ_f (MPa)	K_{Ic}^n (MPa · m$^{0.4878}$)	σ_f (MPa)	K_{Ic}^n (MPa · m$^{0.4555}$)	σ_f (MPa)	K_{Ic}^n (MPa · m$^{0.3843}$)
	12.98	0.608	14.06	0.863	18.52	1.972
	13.49	0.631	13.93	0.855	18.74	1.995
	12.79	0.599	13.87	0.852	18.36	1.955
	12.54	0.587			19.07	2.030
Avg.	12.95	0.606	13.95	0.857	18.67	1.988
St. Dev.	0.40	0.019	0.10	0.006	0.31	0.033

Table 4. Failure strength and critical K_I^n for the notched three-point flexure specimens with $a = 5.33$ mm ($a/h = 0.3$)

	$\gamma = 60°$		$\gamma = 90°$		$\gamma = 120°$	
	σ_f (MPa)	K_{Ic}^n (MPa · m$^{0.4878}$)	σ_f (MPa)	K_{Ic}^n (MPa · m$^{0.4555}$)	σ_f (MPa)	K_{Ic}^n (MPa · m$^{0.3843}$)
	8.40	0.508	11.27	0.884	13.30	1.786
	8.99	0.544	11.52	0.904	14.80	1.989
	8.74	0.529	11.65	0.913	14.73	1.978
	8.99	0.544			14.80	1.989
Avg.	8.78	0.531	11.48	0.900	14.41	1.935
St. Dev.	0.28	0.017	0.19	0.015	0.74	0.100

Table 5. Failure strength and critical K_I^n for the notched three-point flexure specimens with $a = 7.11$ mm ($a/h = 0.4$)

	$\gamma = 60°$		$\gamma = 90°$		$\gamma = 120°$	
	σ_f (MPa)	K_{Ic}^n (MPa · m$^{0.4878}$)	σ_f (MPa)	K_{Ic}^n (MPa · m$^{0.4555}$)	σ_f (MPa)	K_{Ic}^n (MPa · m$^{0.3843}$)
	7.60	0.596	8.80	0.890	9.12	1.584
	7.28	0.571	9.05	0.916	9.66	1.678
	7.09	0.556	9.05	0.916	9.62	1.672
	7.41	0.581			9.81	1.705
Avg.	7.35	0.576	8.97	0.907	9.55	1.660
St. Dev.	0.21	0.017	0.15	0.015	0.30	0.052

5. DISCUSSION

From Tables 2–5 we see that for a given notch angle and notch depth, the measured failure strengths are extremely repeatable. For all of the notch angle/depth combinations the standard deviation divided by the average strength is only 2.2%. The repeatability is slightly better for the $\gamma = 90^\circ$ specimens than for the other two notch angles. Nevertheless, the scatter for all notch angles is far less than that observed in plain strain fracture tests with PMMA where scatter of $\pm 12\%$ is typical (Williams, 1977; 1984). This is probably because the small, but finite, notch angle and notch-tip radius between various specimens is more consistent than that for artificially-induced cracks. Additionally, no craze zone is observed ahead of the notch tip before fracture. For cracks, a craze zone, albeit small, is often observed ahead of the crack tip (Marshall *et al.*, 1973; Williams 1984).

If fracture can be correlated with a critical value of K_I^n, then we can use the specimen dimensions along with the measured failure stress in eqn (6) to compute the critical value of K_I^n, i.e., K_{Icr}^n. If K_{Icr}^n so obtained does not vary with changes in geometry (notch depth in the present case) then it can be used to correlate failure. The average and standard deviations of K_{Icr}^n extracted in this manner are given in Table 6 for $\gamma = 0^\circ$, 60°, 90°, and 120°, respectively. The small variance of K_{Icr}^n obtained from the specimens of four different notch depths (Tables 2–5) strongly suggests that the single parameter K_{Icr}^n can be used to correlate fracture initiation at sharp notches. Although it is apparent that K_{Icr}^n decreases with notch angle, it is reminded that such a comparison is probably not strictly warranted because although the single parameter K_{Icr}^n alone describes the stress state at the notch tip, it describes a different stress state for each notch angle. Indeed the units of K_{Icr}^n differ for each notch angle. Though, while we may be able to correlate K_{Icr}^n for different notch angles empirically, the theoretical basis for such a strict connection is lacking. Along these lines we again mention the work of Carpinteri who attempted to correlate K_{Icr}^n with notch angle. Our results are in general agreement with his in that they show an increase in K_{Icr}^n with γ, and furthermore that, the increase in K_{Icr}^n is slight over $0 \leqslant K_{Icr}^n < \approx 60^\circ$.

That the single parameter K_I^n can correlate fracture initiation for a given notch angle is further demonstrated in Fig. 5 where the failure strength computed using K_{Icr}^n in eqns (6) and (8) is plotted as a function of a/h. The predicted failure strength agrees well with measurements for all three notch angles. This supports the validity of linear elastic notch mechanics (LENM) with a notch fracture toughness criterion for fracture initiation.

In Figures 5a–c we have also shown the predicted failure stresses based on an analysis that approximates the notch as a crack. In other words, we used K_{Icr}^n and $f(a/h)$ for $\gamma = 0^\circ$ along with eqns (6) and (8), to predict the failure stress for the notched specimens with $\gamma = 60^\circ$, 90°, and 120°. The predictions based on the crack solution underestimate the failure stress in each case, and the error increases as γ increases. For $\gamma = 60^\circ$, the difference between the crack and notch solutions is about 20%. It is about 30% for $\gamma = 90^\circ$ and 45% for $\gamma = 120^\circ$. It is apparent that modeling the sharp notch as a crack can lead to substantial error, particularly as the notch angle increases. However, an alternative approach to predict fracture initiation might be to use the solution of eqn (6), along with $f(a/h)$ for a crack. This may be attractive since tabulated values of $f(a/h)$ for a crack exist for many geometries, and the other terms in eqn (6) are obtained simply from dimensional analysis. In this case,

Table 6. Critical K_I^n for the notched three-point flexure specimens as a function of notch angle.†

$\gamma(^\circ)$	K_{Icr}^n (MPa·m$^{1-\lambda}$)	Std. Dev. (MPa·m$^{1-\lambda}$)
0	0.407	0.048
60	0.573	0.031
90	0.886	0.023
120	1.908	0.162

† The fracture toughness reported here is $K_{Icr}/\sqrt{2\pi}$ where K_{Icr} is the traditional plane strain fracture toughness. The difference is due to our definition of K in eqn (5).

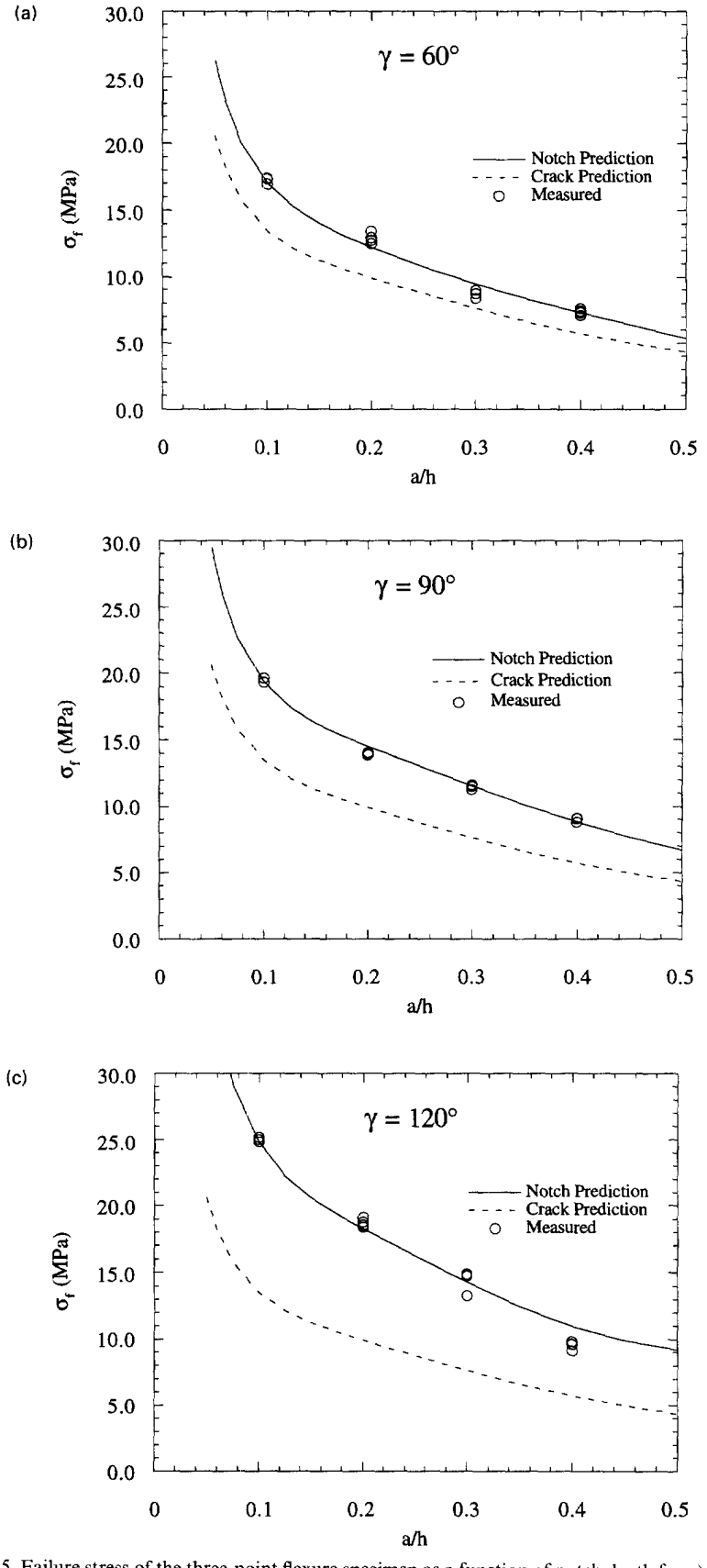

Fig. 5. Failure stress of the three-point flexure specimen as a function of notch depth for a) $\gamma = 60°$, b) $\gamma = 90°$, and c) $\gamma = 120°$. Open circles are measurements and the solid line is the prediction based on a critical K_I^n.

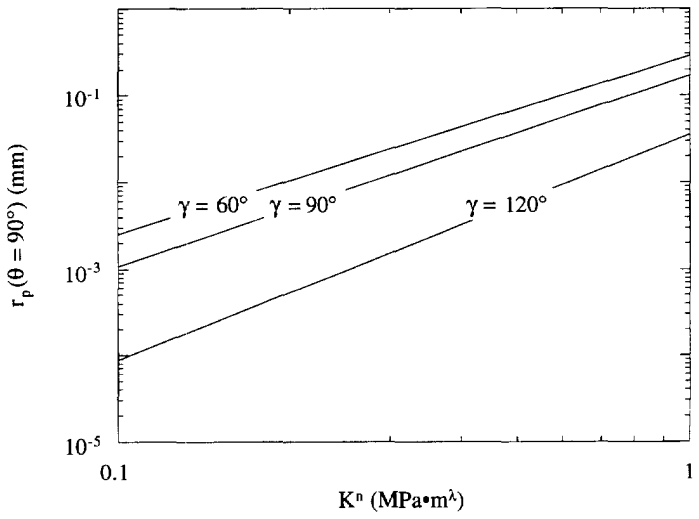

Fig. 6. K_I^n-based estimate of plastic zone size at $\theta = 90°$ vs. applied K_I^n for $\gamma = 60°$, 90°, and 120°.

$f(a/h)$ for crack is less than that for the three notches by roughly 7%, 13%, and 28% for $\gamma = 60°$, 90°, and 120°, respectively.

We also used the linear elastic asymptotic solution to estimate the size and shape of a plastic zone ahead of the notch tip at the measured failure load. We have not attempted to consider the complicated phenomenology of the deformation of PMMA, but as a simple estimate have assumed elastic–plastic behavior. Estimates of the craze zone could be obtained in a similar manner as discussed by Williams (1984) in the context of cracks. Taking a yield stress of $\sigma_y = 51$ MPa and assuming yield initiates when the von Mises effective stress equals σ_y, the size and shape of the plastic zone $r(\theta)$ can be estimated as:

$$r_p(\theta) = \left(\frac{\sigma_y}{K_I^n}\right)^{1/(\lambda-1)} f_e(\theta)^{1/(1-\lambda)}. \tag{10}$$

The von Mises effective stress, based on the asymptotic elastic solution, is expressed as $\sigma_e = K_I^n r^{\lambda-1} f_e(\theta)$ and is computed from the stress components in eqns (3) in the standard manner. Note that $f_e(\theta)$ depends on $f_{rr}(\theta)$, $f_{\theta\theta}(\theta)$, and $f_{r\theta}(\theta)$ and differs depending on whether plane stress or plane strain conditions are assumed. The asymptotic-based estimate of r_p for plane strain conditions at the point of maximum yielding ($\theta = 90°$) is plotted in Fig. 6. For the $\gamma = 90°$ specimens at an applied K_I^n of 0.886 MPa·m$^{0.4555}$ ($= K_{Icr}^n$), $r_p \approx 0.13$ mm. This is much smaller than the region dominated by the singular field for the $a/h = 0.1$ notched bar which is ≈ 2.5 mm as determined by the continuum finite element calculations. For the $a/h = 0.4$ notched bar the region dominated by the singular field is ≈ 0.8 mm which is still substantially larger than r_p. Again, this supports the use of a single parameter description of the stress state at the notch tip and the use of a critical K_I^n as a failure criteria.

6. CONCLUSION

We determined the magnitude of the stress intensity K_I^n for notched mode I three-point flexure specimens using a combination of Williams (1952) asymptotic method, dimensional considerations, and detailed finite element analysis. Our corresponding measurements using a series of notched polymethyl methacrylate (PMMA) three-point flexure specimens with notch angles of 60°, 90°, and 120° demonstrate the feasibility of using a critical value of K_I^n to correlate fracture initiation. Using the measured failure loads and the finite element solutions for K_I^n, we inferred the critical K_I^n for sharp-notched PMMA. Furthermore, we showed that elastic estimates of the plastic zone size for the notched PMMA specimens are small relative to the singularity-dominated zone. This supports the applicability of linear

elastic notch mechanics (LENM), and the contention that a critical value of K_I^n can be used to correlate fracture initiation from sharp notches.

Acknowledgements—The support of Ford Microelectronics Inc. and the National Science Foundation (CMS-9523073) is gratefully acknowledged.

REFERENCES

Berry, J. P. (1961) Fracture process in polymeric materials. I. The surface energy of poly(methyl methacrylate). *Journal of Polymer Science* **50,** 107–115.

Carpinteri, A. (1987) Stress-singularity and generalized fracture toughness at the vertex of re-entrant corners. *Engineering Fracture Mechanics* **26,** 143–155.

Dempsey, J. P. and Sinclair, G. B. (1981) On the singular behavior at the vertex of a bimaterial wedge. *Journal of Elasticity* **11,** 317–327.

Dunn, M. L., Suwito, W. and Cunningham, S. J. (1996) Stress intensities at notch singularities. *Engineering Fracture Mechanics*, in press.

Gross, B. and Mendelson, A. (1972) Plane elastostatics of V-notched plates. *International Journal of Fracture Mechanics* **8,** 267–276.

Gu, L. and Belytschko, T. (1994) A numerical study of stress singularities in a two-material wedge. *International Journal of Solids and Structures* **31,** 865–889.

Higuchi, M. (1958) *Reports of Research, Institute for Applied Mechanics*, Vol. 6, pp. 173–179. Kyushu University, Japan.

Knesl, Z. (1991) A criterion of V-notch stability. *International Journal of Fracture* **48,** R79–R83.

Ledbetter, 1996. Personal correspondence.

Leicester, R. H. (1973) Effect of size on the strength of structures. CSIRO Forest Products Laboratory, Division of Building Research, Paper No. 71.

Marshall, G. P., Culver, L. E. and Williams, J. G. (1973) Article title. *International Journal of Fracture* **9,** 295–309.

Reedy, Jr., E. D. and Guess, T. R. (1993) Comparison of butt tensile strength data with interface corner stress intensity factor prediction. *International Journal of Solids and Structures* **30,** 2929–2936.

Reedy, Jr., E. D. and Guess, T. R. (1995) Butt tensile joint strength: interface corner stress intensity factor prediction. *Journal of Adhesion Science Technology* **9,** 237–251.

Reedy, Jr., E. D. and Guess, T. R. (1996) Butt joint strength: effects of residual stress and stress relaxation. *Journal of Adhesion Science Technology*, in press.

Reedy, Jr., E. D. (1990) Intensity of the stress singularity at the interface corner between a bonded elastic and rigid layer. *Engineering Fracture Mechanics* **38,** 575–583.

Reedy, Jr., E. D. (1991) Intensity of the stress singularity at the interface corner of a bonded elastic layer subjected to shear. *Engineering Fracture Mechanics* **38,** 273–281.

Reedy, Jr., E. D. (1993a) Asymptotic interface corner solutions for butt tensile joints. *International Journal of Solids and Structures* **30,** 767–777.

Reedy, Jr., E. D. (1993b) Free-edge stress intensity factor for a bonded ductile layer subjected to shear. *Journal of Applied Mechanics* **60,** 715–720.

Sinclair, G. B., Okajima, M. and Griffin, J. H. (1984) Article title. *International Journal for Numerical Methods in Engineering* **20,** 999–1008.

Sukumar, N. and Kumosa, M. (1992) Application of the finite element iterative method to cracks and sharp notches in orthotropic media. *International Journal of Fracture* **58,** 177–192.

Ting, T. C. T. and Chou, S. C. (1981) Edge singularities in anisotropic composites. *International Journal of Solids and Structures* **17,** 1057–1068.

Ting, T. C. T. (1986) Explicit solution and invariance of the singularities at an interface crack in anisotropic composites. *International Journal of Solids and Structures* **22,** 965–983.

Walsh, P. F. (1974) Linear fracture mechanics solutions for zero and right angle notches. CSIRO Forest Products Laboratory, Division of Building Research, Paper No. 2.

Walsh, P. F. (1976) Crack initiation in plain concrete. *Magazine of Concrete Research* **28,** 37–41.

Williams, J. G. (1977) Fracture Mechanics of Polymers. *Polymer Engineering Science* **17,** 144–149.

Williams, J. G. (1984) *Fracture Mechanics of Polymers*. Ellis Horwood, Chichester.

Williams, M. L. (1952) Stress singularities resulting from various boundary conditions in angular corners of plates in extension. *Journal of Applied Mechanics* **74,** 526–528.